

Quantitative Prediction of Deformed Austenite and Transformed Ferrite Texture in Hot-rolled Steel Sheet

Yasuaki TANAKA*

Toshiro TOMIDA

Abstract

To achieve quantitative and continuous prediction of textures through the deformation and phase transformation during hot rolling of steel, the integration of the Taylor type crystal plasticity model, called "Grain Interaction model (GIA)", and the transformation texture model, called "Double Kurdjumov-Sachs relation (DKS)", has been investigated. The deformed austenite (γ) texture is predicted by GIA with taking into account not only the standard $\{111\}\langle 110 \rangle$ slip system but also non-octahedral slip systems. Then the transformed α texture is calculated by DKS, in which a nucleated α prefers to have an orientation relationship near the K-S relation with both of two neighboring γ grains. For validation, single pass hot-rolling test of a C-Si-Mn steel was carried out to prepare steel sheets with some amounts of retained austenite, and then the ferrite texture observed by X-ray diffraction was compared with the simulated texture by the above methods. The comparison between the predicted and the experimental textures shows that the linked model (GIA & DKS) can lead to a remarkable reproduction of the texture of hot-rolled steel sheets.

1. Introduction

Texture has significant influence on the properties of steel sheets. Controlling textures is an important task in manufacturing steel sheets, along with the issues of microstructures. As texture changes every moment during the manufacturing processes up to that of the end products, it is important to understand the processes of texture development under manufacture in order to control them. It is difficult to directly observe actual texture development during the manufacturing processes, which is why the prediction by means of a numerical model is considered promising.

In addition to the use as-is as finished products, hot-rolled steel sheets are further processed in the cold rolling and annealing processes to be used as cold-rolled steel sheets. Texture formed in a process is taken over by the following manufacturing processes one by one, influencing the next process. Therefore, in order to have finished products with desirable properties, we should first have the ability to predict the development processes of the texture of hot-rolled steel sheets.

However, how the textures of hot-rolled steel sheets develop has not been fully understood because steel sheets go through sol-

id-phase transformation in the cooling process after being hot rolled at high temperatures. No one has succeeded in predicting textures throughout the entire processes in a quantitative way. Furthermore, in addition to the complexity of manufacturing processes, which consist of processes in equipment including a heating furnace, many hot rolling stands, and cooling zones, operation conditions vary depending on product types. Therefore, approaches using experience models or quantification are practically difficult. For that reason, for quantitative prediction of texture throughout the entire manufacturing processes, it is necessary that texture development processes are separated from the viewpoint of metallurgy, a model is formulated for each elementary process based on physical laws, and one process is linked to another.¹⁾ Such method is being examined for the application to steel.²⁾

The development processes of steel texture are broadly divided into deformation, recrystallization, and transformation. In this study, we try to quantitatively predict hot-rolled steel sheet texture after deformation and transformation by linking the crystal plasticity model with the variant selection model.

* Senior Researcher, Fundamental Metallurgy Research Lab., Advanced Technology Research Laboratories
1-8 Fuso-cho, Amagasaki, Hyogo Pref. 660-0891

2. Body

2.1 Simulation models

2.1.1 Deformation texture prediction model

To predict the texture of deformed austenite γ , a Taylor type crystal plasticity model called the grain interaction model (GIA)³⁾ was used. The GIA, which is different from standard Taylor models, can handle slip and rotation of a crystal grain taking into account adjacent crystal grains.

Figure 1²⁾ shows a sample model consisting of gathered aggregates. An aggregate is considered to consist of eight crystal grains. When the sample is deformed, these aggregates deform along the plastic deformation route in the entire sample as is the case with a standard Taylor model. However, the deformation of each crystal grain in the aggregates does not need to accord with the strain of the sample. When such free deformation is assumed for crystal grains in the aggregates, the shapes of crystal grains do not accord with each other at the boundary faces. Therefore, the concept of geometrical necessary dislocations (GNDs) is introduced to guarantee the continuity of material of an interface at which crystal grains do not align with the shape.

The crystal plasticity model is used to predict the development of deformation texture based on the assumption of the slip and rotation of crystal grains caused by deformation externally applied. For such processing, a slip system that works in each crystal grain needs to be determined. While in a Taylor model, a combination of slip systems in which deformation energy becomes minimum is calculated, in the GIA, the slip system for each crystal grain in the aggregates is determined such that the total of the deformation energy (first term) and the energy to introduce GNDs (second term) becomes minimum as shown in equation (1).

$$E_{total} = \sum_{k=1}^8 \sum_{s(k)=1} |\dot{\gamma}_k^s| \tau_{crit,k}^s + \sum_{k=1}^8 \sum_{GBs,IFs} E_{GND} = minimum \quad (1)$$

Which slip system is actually selected is dependent on the predetermined candidates for slip systems, their maximum critical shearing stress (CRSS), and work-hardening rules of the material. For candidates for slip systems in this study, in addition to $\{111\}\langle 011 \rangle$, which are the closest-packed plane and closest-packed direction of face centered cubic (FCC), $\{011\}\langle 011 \rangle$ and $\{112\}\langle 110 \rangle$ were selected as possible slip systems while introducing the concept of non-closest-packed plane slips in view of the fact that the material is hot rolled at a high temperature. Regarding non-closest-packed plane slips in hot working, whereas reports have already been made for mainly aluminum alloys, the CRSS values described in these reports vary in a wide range from 0.75 to 1.4 compared to closest-packed plane slip values, remaining uncertain.⁴⁻⁶⁾ Therefore, in this study, the CRSS of a non-closest-packed plane slip is assumed as equal to that of closest-packed plane slip for calculation.

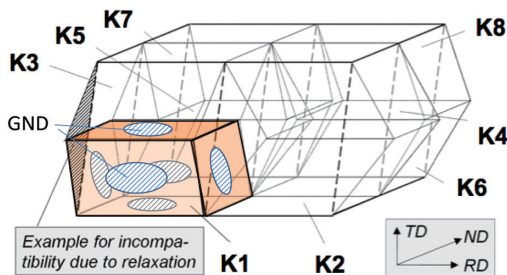


Fig. 1 8-grain aggregate described in the GIA model²⁾

In addition, in order to consider work-hardening rules of the material in hot working, a work-hardening model that relies on the strain rate was linked to the GIA. Although we cannot go into detail here due to the space limitations of this paper, parameters of the work-hardening model were determined such that they accorded with the thermal stress/strain properties obtained in a hot compression test (Formaster test).

When investigating focusing on the center of thickness of the hot-rolled steel sheets, the plastic strain in the sample increases along the plane strain deformation. When precise plane strain deformation is applied to a Taylor type crystal plasticity model, the obtained deformation texture at the center of the thickness is significantly sharper than the actual texture. To solve such issue of inconsistency, it was proposed to allow the increment of plastic strain in a sample to be different from the ideal plane strain deformation and to introduce shear components.⁷⁾ In line with this approach, we used tensors of strain increments proposed by Engler⁷⁾ shown in equation (2). These values were randomly used in each calculation step within the range allowed for each element, thereby predicting the development of rolled deformation textures.

$$\begin{aligned} \dot{\epsilon}_{11} &= 1 \pm 0.1, \quad \dot{\epsilon}_{33} = -1 \pm 0.1, \quad \dot{\epsilon}_{22} = -\dot{\epsilon}_{11} = \dot{\epsilon}_{33}, \\ \dot{\epsilon}_{13} &= 0 \pm 0.6 \dots 0.75, \quad \dot{\epsilon}_{23} = 0 \pm 0.4, \quad \dot{\epsilon}_{12} = 0 \pm 0.3 \dots 0.15 \quad (2) \end{aligned}$$

The prediction calculation (simulation) was performed for 4000 crystal grains with random distribution of orientations using the strain speed and reduction of the cross-sectional area that were the same as those used in the rolling test explained later. The obtained discrete orientations of the crystal grains after deformation were used to calculate the orientation distribution function (ODF). Then the texture was compared to those obtained in the test and was also used in the transformation texture model described later.

2.1.2 Transformation texture model

An α phase precipitated from a certain γ phase in steel has specific crystal orientation relationships with the γ phase, including the Kurdjumov-Sachs (K-S) relationship. The Kurdjumov-Sachs (K-S) relationship is represented as $\{111\}\gamma // \{011\}\alpha$ and $\langle 011 \rangle\gamma // \langle 111 \rangle\alpha$. In both γ and α phases, the closest-packed planes and closest-packed orientations before and after the transformation are respectively parallel to each other. As the crystal structures of both γ and α phases are cubic crystals, there are 24 combinations (variants) that are crystallographically equivalent in the K-S relationship. However, as actually some of these variants are preferentially selected, consideration for variant selection rules is essential for quantitative prediction of the transformation texture. In this study, the double K-S relations model (DKS) proposed recently^{8,9)} was used to predict the transformation texture. The DKS has been reported as capable of quantitatively reproducing the transformation texture in low C-Mn steel.

This model is, as shown in **Fig. 2**, based on the assumption of the priority of a variant in a double K-S relationship; in other words, a variant that has an orientation close to the K-S relationship with the adjacent γ grains on both sides when nucleation of the α phase occurs on the grain boundaries of the γ grains. As grain boundaries that can have strict K-S relationships with both γ grains are limited to extremely special cases, it is almost impossible for such grain boundaries to occur. However, if deviation from the K-S relationship by approximately 10° is allowed at the interface between the α phase and at least a γ on one side, the DKS hypothesis is possible at any grain boundary.

As shown in **Fig. 2**, in order for a certain variant i to be selected

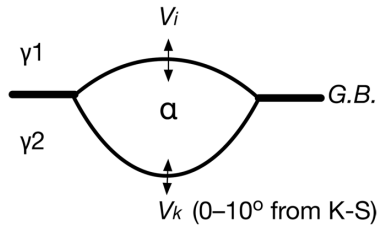


Fig. 2 Schematic image of α nucleate on the γ grain boundary with double K-S relation

at the γ_1 - α interface (on one side) in accordance with the DKS, there must be another variant k at the α - γ_2 interface (on the other side). In other words, the probability in which α is precipitated with variant i from γ_1 is proportional to the orientation density of γ_2 . A variant selection function that expresses this is:

$$\rho(g) = \frac{\omega}{N} \sum_k f(\Delta g^{-1} \cdot g_k^c \cdot \Delta g \cdot g) + \rho_c(g) \quad (3)$$

When closely scrutinizing equation (3), the variant selection function is the sum of a portion (first term) that is formed in accordance with the DKS and another (second term; $\rho_c(g)$) that does not involve variant selection here other than the DKS. In this function, Δg is the orientation change as a result of $\gamma \rightarrow \alpha$ transformation. When changes in lattice constants are ignored, a simple rotation matrix can indicate Δg . g_k^c is a rotation matrix based on cubic symmetry. g_k^c and Δg represent variant changes. ω is a constant to determine the intensity of the DKS rule. In this study, ω was determined such that the α texture obtained from the test accords with the value computationally predicted. N is the total number of variants to be considered.

Generally, texture can be indicated as equation (4) using the spherical harmonic expansion method. The expansion coefficient ${}^a C_{\lambda}^{\mu\nu}$ for α after the transformation can be calculated using expansion coefficient ${}^{\gamma} C_{\lambda}^{\mu\nu}$ for γ texture before the transformation and variant selection coefficient $\rho_{\lambda_2}^{\nu_2}$ as shown in equation (5).¹⁰⁾ $\hat{T}_{\lambda}^{\mu\nu}$ is the basis function in consideration of crystal symmetry and $\hat{A}_{\lambda_1}^{m_1\mu}$ is its symmetry coefficient. Furthermore, $(\lambda_1 \lambda_2 m_1 \mu | \lambda s)$ is a Clebsch-Gordan coefficient and $\{\lambda_1 \lambda_2 \nu_1 \nu_2 | \lambda \nu\}$ is a coefficient redefined by Bunge, et al.¹⁰⁾ in consideration of the symmetry of the basis function. $\rho_{\lambda_2}^{\nu_2}$ is a coefficient that can be obtained by expanding the aforementioned variant selection function $\rho(g)$ using basis function $\hat{T}_{\lambda}^{\nu_2}$ in which the sample symmetry is considered as shown in equation (6). It includes an expansion coefficient for the parent γ phase. This shows that the variant selection rules are influenced by the γ texture itself before the transformation in the DKS model.

$$f_{\alpha}(g) = \sum_{\lambda=0}^{\infty} \sum_{\mu=1}^{M(\lambda)} \sum_{\nu=1}^{N(\lambda)} {}^a C_{\lambda}^{\mu\nu} \hat{T}_{\lambda}^{\mu\nu}(g) \quad (4)$$

$${}^a C_{\lambda}^{\mu\nu} = \sum_{\lambda_1=0}^{\infty} \sum_{\mu_1=1}^{M(\lambda_1)} \sum_{\nu_1=1}^{N(\lambda_1)} {}^{\gamma} C_{\lambda_1}^{\mu_1\nu_1} \left[\sum_{\lambda_2=0}^{\infty} \sum_{\nu_2=1}^{N(\lambda_2)} \rho_{\lambda_2}^{\nu_2} \hat{A}_{\lambda_1}^{m_1\mu} (\lambda_1 \lambda_2 m_1 \mu | \lambda s) \{ \lambda_1 \lambda_2 \mu_1 \mu_2 | \lambda \nu \} \hat{T}_{\lambda}^{\mu\nu*}(\Delta g) \right] \quad (5)$$

$$\rho_{\lambda_2}^{\nu_2} = \frac{\omega}{N} \sum_{\mu=1}^{M(\lambda_2)} {}^{\gamma} C_{\lambda_2}^{\mu\nu_2} \left[\sum_k \hat{T}_{\lambda_2}^{\mu\nu*}(\Delta g^{-1} \cdot g_k^c \cdot \Delta g) - \frac{1}{24} \sum_{i,k} \hat{T}_{\lambda_2}^{\mu\nu*}(\Delta g^{-1} \cdot g_k^c \cdot \Delta g \cdot g_i^c) \right] \quad (6)$$

2.2 Validation of the prediction models

To validate the quantitativity of the prediction models, we conducted laboratory hot rolling tests as follows. First, steel containing chemical components of 0.2%C-1.5%Si-1.45%Mn (% by weight) was produced using a vacuum melting furnace to obtain ingots. After that, these ingots were rolled and heat treated to produce 4.9- and 6.8-mm steel sheets as materials in which the ODF random strength ratio was 1.2-fold at maximum and thereby practically no texture

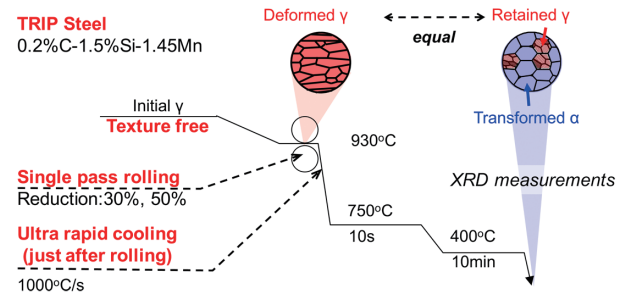


Fig. 3 Schematic representation of experimental hot-rolling

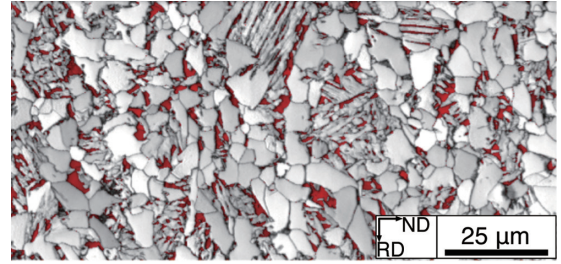


Fig. 4 Phase map of the steel sheet after 50% hot-rolling and transformation²⁾
Red filled area corresponds to the retained γ phase.

was developed.

These material steel sheets were put in a furnace with an N_2 -purged atmosphere at 1000°C for one hour. As shown in Fig. 3, after they are taken out from the furnace each sheet was rolled at a single stand to 30% and 50% reduction to obtain 3.4-mm hot rolled steel sheets. The finish hot rolling temperature was 930°C. Compulsory cooling devices installed immediately downstream of the rolling machines were used to cool the sheets at 1000°C/s immediately after the hot rolling to suppress the recrystallization. To deposit ferrite, the cooling was stopped at 750°C and then the sheets were air-cooled for 10 seconds. After that, the cooling by the cooling devices resumed at 40°C/s until the sheets temperature dropped to 400°C, at which the sheets were held for 10 minutes to stabilize the retained γ .

Figure 4 shows the result of an analysis in which a sample of the texture obtained was analyzed using the electron backscatter diffraction (EBSD). The texture consisted of approximately 8% retained γ , ferrite, bainite, and a very small amount of martensite.

The center of the thickness of the hot rolled steel sheets was cut out. The X-ray diffraction method (XRD) was used to measure incomplete pole figures for BCC and FCC. These pole figures were used to calculate the ODF based on the series expanding method¹¹⁾ and the texture was examined.

In this study, it was assumed that the texture of the retained γ would accord with that of the hot rolled γ before the transformation in order to validate the predictive calculation.

2.3 Model validation test results and consideration

2.3.1 Prediction simulation for deformation textures

Figure 5 shows an ODF comparison result of the γ texture of the 30% hot-rolled steel sheet obtained in the test to that obtained by GIA predictive calculation. The measured γ texture obtained in the test is similar to the typical deformation texture of pure copper after cold rolling. It indicates that the texture of the remaining γ almost accords with the γ texture before the transformation. This result shows that the predictive calculation that considers both clos-

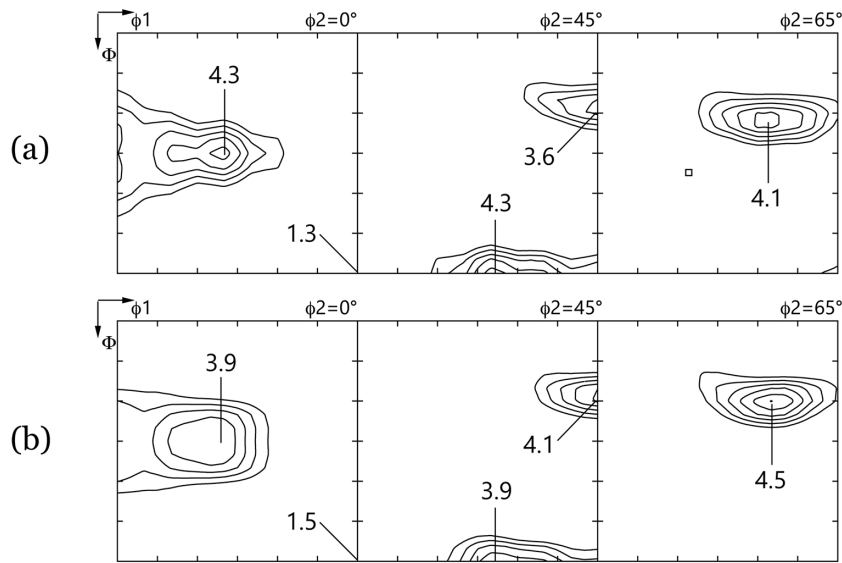


Fig. 5 (a) Measured ODF of the retained γ hot-rolled by 30% in reduction and (b) Predicted textures with octahedral and non-octahedral slip system²⁾

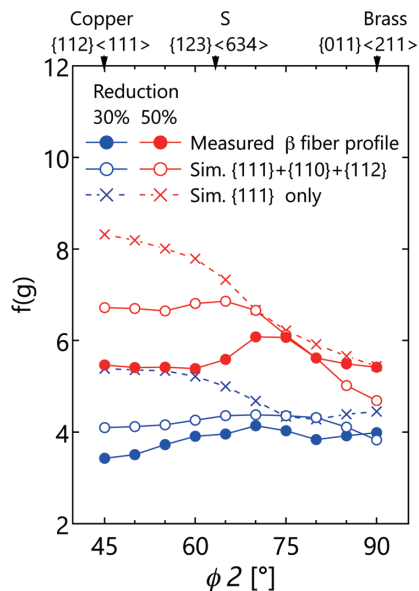


Fig. 6 Comparison of the β fiber intensities between the measured and the simulated textures²⁾

est-packed and non-closest-packed plane slips reproduces the measured deformation texture well.

Furthermore, regarding the texture of the steel sheets hot rolled at different reduction rates, Fig. 6 shows a comparison result between β -fiber intensity profiles along ϕ_2 using values measured in the test and those obtained by the predictive calculation. Both measured and simulated values overall show that texture developed more at the higher reduction rate. Among the simulated values, when only the closest-packed plane slip was taken into account, extremely highly-accumulated intensity occurred in the orientations from S to Copper for both reduction rates and they are significantly diverged from the measured values.

When non-closest-packed plane slips were considered along with the closest-packed plane slips, excessive intensity accumula-

tion in the vicinity of the Copper orientation was suppressed compared to the results obtained when the closest-packed plane slip alone was considered, showing that the simulated values were able to accord with the measured values relatively well.

Currently, when the reduction rate is high, slightly larger intensity accumulation in the orientation of Cu than the measured results is still expected. However, as Copper and Brass orientations relatively strongly rely on CRSS of non-close-packed plane slip systems, the quantitative prediction will possibly be further improved when the investigation of such CRSS is progressed going forward.

The texture of the deformed γ obtained through the processes as described above was used as the parent phase in the transformation texture model in the next section.

2.3.2 Deformation/transformation texture simulation using linked prediction models

Figure 7(a) shows the ODF of the measured α texture. The main orientations of the texture are $\{112\}\langle 110\rangle$ to $\{113\}\langle 110\rangle$ in α -fiber (RD// $\langle 110\rangle$) that appeared on the cross section of $\phi_2 = 45^\circ$, which indicates that it is texture transformed from non-recrystallized γ . This is not inconsistent with the aforementioned deformed γ texture obtained both in the test and predictive calculation.

The deformed γ texture that was calculated above and shown in Fig. 5(b) was used as the parent phase to simulate the α texture using the DKS model. Figure 7(b) shows the result. These figures show that the GIA-DKS-linked model reproduces the measured α texture after the deformation/transformation quite well.

When simulating the texture above, constant ω in equation (3) was determined as 0.8 ($\omega = 0.8$) such that the root mean square of the difference between the measured values for the orientations and the values for the texture simulated using the linked prediction model becomes minimum.

Figure 8 shows a comparison result between the measured and simulated intensities in the vicinity of the main orientations of the texture of BCC α -fiber. The figure shows that the transformation texture calculated without considering variant selection is weaker than the measured texture, indicating that the variant selection rules are required to be taken into account for the quantitative prediction of the transformation texture.

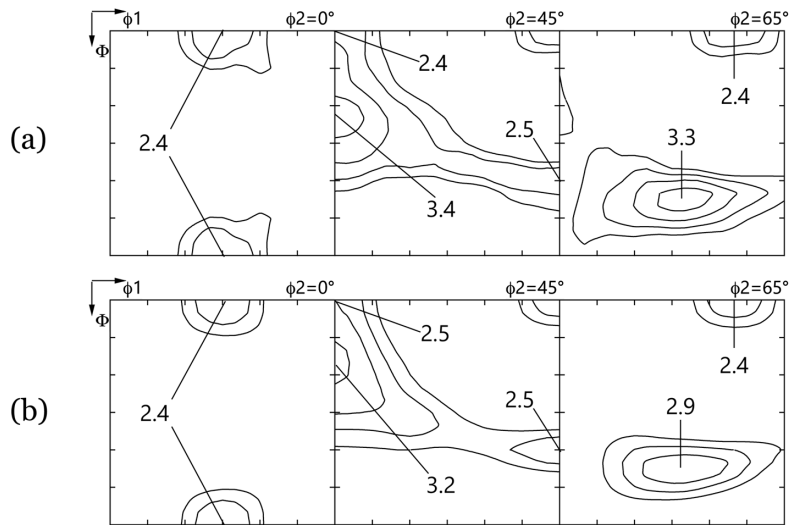


Fig. 7 (a) Experimental textures of the transformed α in hot-rolling steel sheet of 30% reduction, and (b) Prediction by the linked simulation of GIA and DKS. (levels: 1.5, 2.0, 2.5 ...)²⁾

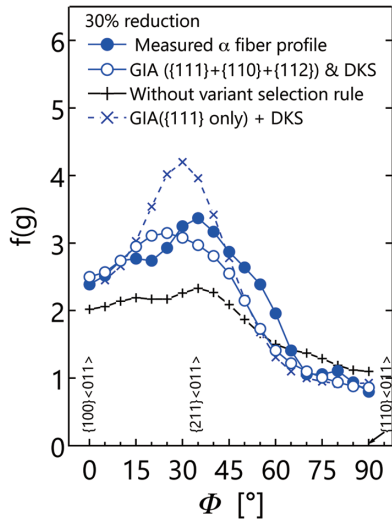


Fig. 8 Measured and the simulated profiles of the BCC α fiber²⁾

The GIA-DKS linking calculation without considering a non-closest-packed plane results in stronger α -fiber than the measured results. This inconsistency with the measured results is due to excessive accumulation in the Copper orientation caused in the deformed γ texture obtained in calculation when no non-closest-packed plane was considered.

As described above, consideration of non-closest packed plane slips in view of hot working can suppress excessive intensity accumulation in the Copper orientation. In particular, as CRSS values for the non-closest-packed plane slips in the $\{112\}\langle 110\rangle$ system have relatively strong influence on the density in orientations of Cu and Brass,⁴⁾ it is important going forward to correctly assign these CRSS values in order to improve the quantitative prediction performance of simulation models. As shown in equation (6), variant selection itself is influenced by the γ texture of the parent phase in the DKS model. Therefore, for further improving the accuracy of linked models for texture transformed in the hot rolling, improving the accuracy of quantitative prediction for the γ texture deformed in hot work-

ing is important.

3. Conclusion

We undertook the development of linked models that are capable of quantitatively predicting deformation/transformation texture of hot-rolled steel sheets. In this study, the concept of non-closest-packed plane slips was introduced into the crystal plasticity model GIA where deformation interaction of adjacent grains was considered. This made it possible to predict γ texture deformed in hot-working in a quantitative way. In addition, such results were linked to the variant selection model DKS, which made it possible to more quantitatively predict α textures after deformation/transformation. Such results indicate the possibility of predicting texture coherently during the entire hot rolling process by the linkage with the recrystallization model in deformed γ .

In addition to the statistical approaches as shown in this study, there are detailed models among the methods for predicting texture using numerical calculation. Such models can cope with local crystal orientations (e.g., location information) and changes in texture.^{12, 13)} In general, such detailed models involve high calculation costs, which currently makes it difficult to predict texture in a sample during the entire hot rolling. However, they are useful for following local orientation changes that statistical models cannot handle, and also for understanding the mechanisms based on the results obtained. We will continue to develop models that can predict coherent texture, using the advantages of both statistical and detailed models.

References

- 1) Gottstein, G. et al.: Materials Science Forum. 519, 93 (2006)
- 2) Tanaka, Y. et al.: Materials Science and Engineering. 82 (1), 012057 (2015)
- 3) Crumbach, M. et al.: Proc. First Joint Int. Conf. Recrystallization and Grain Growth. 1, 2001, p.1053
- 4) Bacroix, B. et al.: Textures and Microstructures. 8, 267 (1988)
- 5) Maurice, C. et al.: Advanced Engineering Materials. 45 (11), 4639 (1997)
- 6) Pérocheau, F. et al.: International Journal of Plasticity. 18 (2), 185 (2002)
- 7) Engler, O.: Advanced Engineering Materials. 4 (4), 181 (2002)
- 8) Tomida, T. et al.: Materials Processing and Texture. 200, 325 (2008)
- 9) Tomida, T. et al.: Acta Materialia. 61 (8), 2828 (2013)
- 10) Bunge, H. J. et al.: Scripta Metallurgica. 17 (12), 1403 (1983)

- 11) Bunge, H. J.: Quantitative Texture Analysis. London, Butterworths, 1982
- 12) Suwa, Y.: Computational Materials Science. 44 (2), 286 (2008)
- 13) Suwa, Y. et al.: CAMP-ISIJ. 28, 891 (2015)



Yasuaki TANAKA
Senior Researcher
Fundamental Metallurgy Research Lab.
Advanced Technology Research Laboratories
1-8 Fuso-cho, Amagasaki, Hyogo Pref. 660-0891



Toshiro TOMIDA
Executive General Manager, Dr. Eng
Amagasaki Unit
Nippon Steel & Sumikin Technology Co., Ltd.